

Effect of Thermal Degradation on the Mechanical Properties of a Diglycidyl Ether of Bisphenol A/1,3-Bisaminomethylcyclohexane (DGEBA/1,3-BAC) Epoxy Resin System

L. BARRAL, J. CANO, J. LÓPEZ, P. NOGUEIRA, C. RAMÍREZ

E. U. P Ferrol, Departamento de Física, Universidad de A Coruña, Cra. de Aneiros s/n, 15405 Ferrol, Spain

Received 28 March 1996; accepted 8 September 1996

ABSTRACT: The effect of thermal degradation on the mechanical properties of a diglycidyl ether of bisphenol A (DGEBA)/1,3-bisaminomethylcyclohexane (1,3-BAC) epoxy system, cured with two different curing cycles—a short cycle and a long cycle—were studied using tensile and Izod impact experiments and scanning electronic microscopy, SEM, observations. From these experiments it can be noted a loss of mechanical properties of the material cured with both cycles with aging time, although the material cured with the long cycle presents better properties at any aging time. This better behavior can be explained from the time temperature transformation, TTT, diagram of this system. A good correlation was observed between the decrease in the intensity of the peak of β transition in $\tan \delta$ curve obtained by dynamic mechanical analysis, DMA, and the decrease of the Izod impact strength when thermal aging is increasing. Also, a good correlation can be found between the increase in the fragility of the material with aging time and the morphology of fractured surfaces observed by SEM. © 1997 John Wiley & Sons, Inc. *J Appl Polym Sci* **63**: 1841–1849, 1997

Key words: epoxy resin; thermal degradation; tensile and Izod impact tests; fractography

INTRODUCTION

The relative size of the market for epoxy resins shows that they are important industrial polymers¹.

As a result of their superior mechanical properties, low shrinkage, and thermal stability, epoxy resins are finding increasing use in a wide range of engineering applications, many of which involve high added value products.

The life of an epoxy resin is influenced by a

number of time dependent phenomena. One of these is the generic category of aging, which includes physical, chemical, and mechanical aging.

Thermal degradation is a kind of chemical aging. Chemical aging involves crosslinking reactions. Because these reactions occur as a result of the presence of unreacted species, they will continue for a long time, continuously changing material properties.² These changes can be followed using different techniques. Recently, a considerable amount of research has been done on the thermal degradation of epoxy resins because this is a major problem in the application of these materials in different types of environments.^{3–5}

In the laboratory, thermal degradation can be studied by several kinds of test. Most commonly,

Correspondence to: L. Barral.

Contract grant sponsor: Xunta de Galicia.

Contract grant number: XUGA 17201A92.

© 1997 John Wiley & Sons, Inc. CCC 0021-8995/97/131841-09

samples of a polymer system are aged at an elevated temperature in nitrogen, air, or oxygen. Changes in structure may be inferred from changes in physical properties such as tensile modulus or elongation at break on aging.⁶

In previous works^{7,8} we have studied the thermal degradation of the diglycidyl ether of bisphenol A/1,3-bisaminomethylcyclohexane (DGEBA/1,3-BAC) epoxy system using dynamic mechanical analysis (DMA) and differential scanning calorimetry (DSC). The objective of this work was to analyze the effect of thermal degradation on the mechanical properties of this system employing mechanical techniques (tensile and Izod impact tests), and fractography.

Fractography is very useful to examine the fracture surface of a failed component and to determine the cause of failure, initiation site, direction of crack propagation, state of stress or loading conditions, effect of environmental exposure, material defects, or processing deficiencies.⁹

On the other hand, the different transformations observed during the cure of the DGEBA/1,3-BAC system may be condensed in a time temperature transformation (TTT) diagram. This diagram is an useful tool for analyzing and designing curing processes of thermosetting systems. The diagram is based on the phenomenological changes that take place during cure such as vitrification and gelation. In this article we try to interpret the mechanical properties of this system with the aid of the TTT diagram.

EXPERIMENTAL

Materials

The epoxy resin used was a diglycidyl ether of bisphenol A (DGEBA), Shell Epikote 828, with weight per epoxy equivalent, WPE = 192.2 g/Eq as determined by hydrochlorination.¹⁰ The curing agent was a cycloaliphatic diamine, 1,3-bisaminomethylcyclohexane (1,3-BAC), from Mitsubishi Gas Chem. Co., with molecular weight of 142.18 and manufacturer purity value of > 99%. Both components were commercial products, and they were used as received without purification. The formulation used was 100 g DGEBA to 18.5 g 1,3-BAC.

In order to allow the evacuation of air bubbles the epoxy prepolymer and the hardener were stirred under vacuum at room temperature for 10

min, and then poured into a rectangular mold to obtain a homogeneous sheet of the material. The mixture was subjected to two different curing cycles. A short cycle consists of 24 h at room temperature followed by 2 h at 120°C, and a long cycle consists of 24 h at room temperature followed by 8 h at 60°C, and a postcure of 2 h at 120°C.

Then, from the cured material the samples were cut for the tensile and Izod impact tests, according with their corresponding ASTM standards. For the analysis of thermal degradation the samples were aged in forced air convection oven set at 156°C, a temperature above the maximum glass transition temperature, $T_{g^{\infty}} \approx 150^{\circ}\text{C}$, determined for this epoxy system.¹¹

Tensile and Izod Impact Tests

Tensile properties were measured using a Lloyd Instruments testing machine (model L 6000 R) according to low strain rate tensile testing method as per ASTM D638.¹² All tests were made at room temperature and at a crosshead speed of 5 mm/min.

The samples for the tensile measurements were cut in the standard dumbbell shape. Some samples were tested without degradation but the greater part of them were tested after different lengths of aging time.

Izod impact tests were performed at room temperature in a JBA 16975 impactor using notched samples, according to ASTM D256 standard.¹³

Scanning Electronic Microscopy (SEM)

Phase morphology of DGEBA/1,3-BAC samples was examined using a JEOL JXA-6400 SEM computerized scanning electron microscope. The fracture surfaces of the samples undergoing failure in tensile testing were used as specimens after coating with a thin layer of gold using a high vacuum gold sputterer Balzers SCD 004.

RESULTS

Tensile Tests

Tensile properties such as tensile strength, percent elongation at break, and tensile modulus were measured with the above mentioned testing machine.

Five samples for each aging time were taken

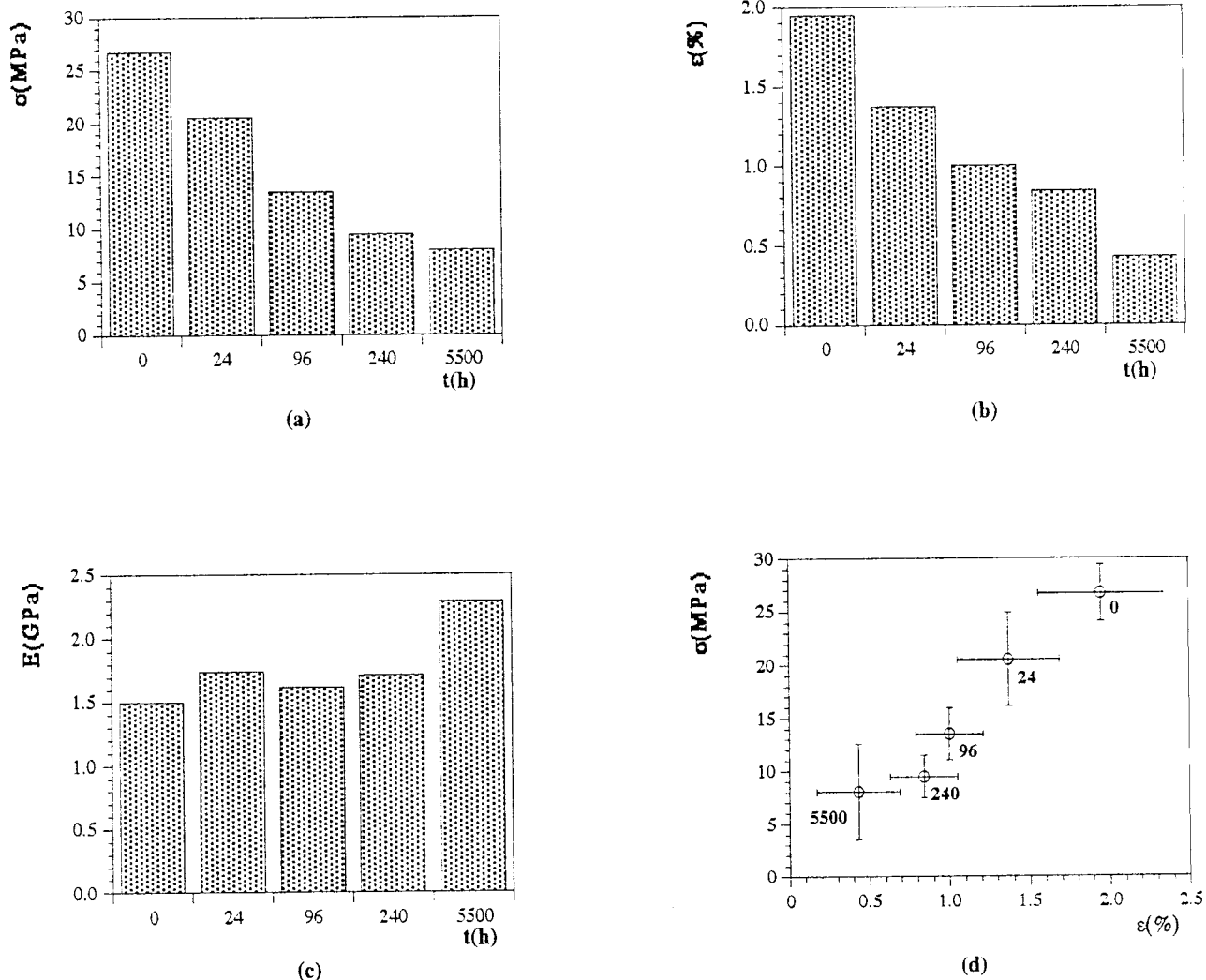


Figure 1 Tensile properties vs. aging time for the material cured with the short cycle.

out of the oven and then tested. The data reported are averages of the five measurements.

The material cured with the short cycle was tested without degradation and with 24, 96, 240, and 5500 h of aging time. The values of tensile strength, σ , percent elongation at break, ϵ , and tensile modulus, E , are shown respectively in Figure 1(a), (b), and (c), for the different aging times. Figure 1(d) shows in the stress-strain plane the break points, where the numbers below each experimental point indicate hours of thermal degradation. It can be observed that the values of σ and ϵ decrease with increasing aging time, while no appreciable trend is observed for the value of E .

The material cured with the long cycle was

tested without degradation and with 24 and 240 h of aging time. Figure 2 shows the comparison between the tensile properties for the two different curing cycles. It is clearly observed from this figure that the values of σ and ϵ decrease with increasing aging time for the two curing cycles, although the material cured with the long cycle shows higher values of σ and ϵ than the material cured with the short cycle for the same aging time. The trend in the value of E is not clear but it is appreciably higher than the value of E for the material cured with the short cycle.

Izod Impact Tests

Ten samples for each aging time were taken out of the oven and then tested. The data reported

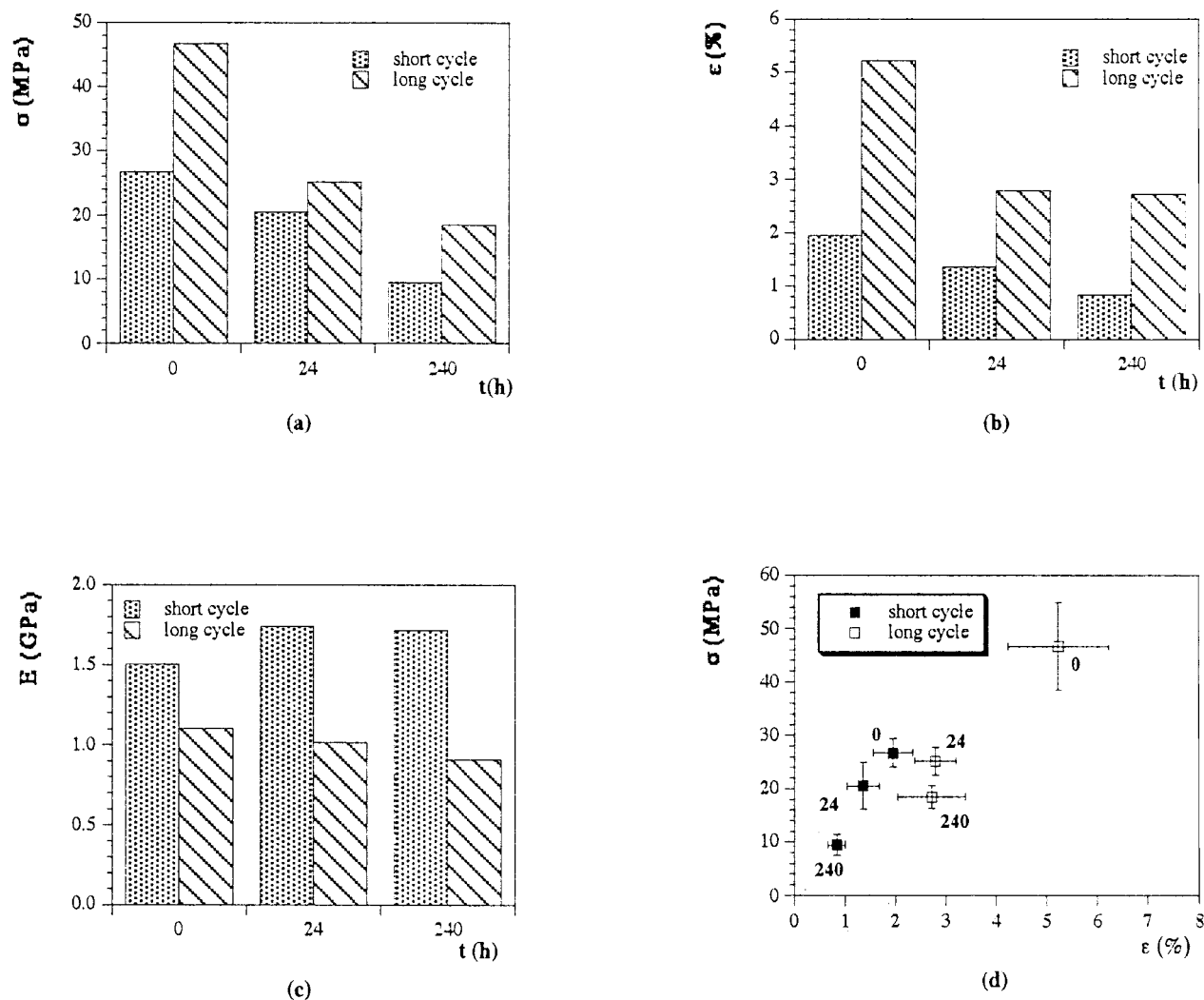


Figure 2 Comparison of tensile properties vs. aging time for the material cured with both cycles.

are averages of 10 measurements with their corresponding standard deviations.

The material cured with the long cycle was tested without degradation and with 24, 240, and 4700 h of thermal degradation. Table I summarizes the values obtained of the Izod impact strength for the different aging times for this material.

The material cured with the short cycle was tested without degradation and with 240 h of thermal degradation. Figure 3 illustrates the comparison between the Izod impact strength for the material cured with the two cycles. It can be noted that there is a decrease in the value of the Izod impact strength when thermal aging is increasing for the two cycles, and also the material cured

with the long cycle presents a higher value of the Izod impact strength than the material cured with the short cycle for the same aging time.

Table I Izod Impact Strength for the Different Aging Times for the Material Cured with the Long Cycle

Time (h)	Izod Impact Strength (J/m)	Standard deviation (J/m)
0	49.03	10.82
24	41.36	4.37
240	38.33	6.42
4700	21.92	2.31

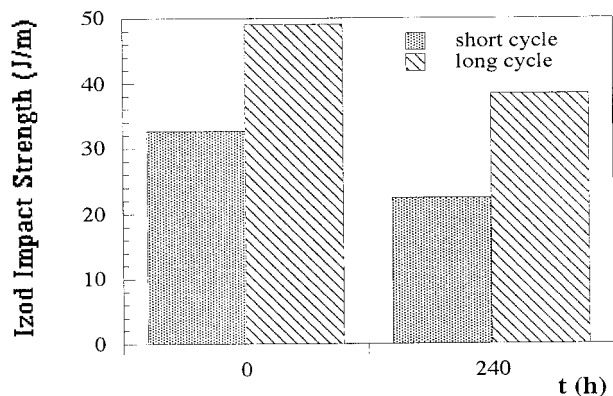


Figure 3 Izod impact strength vs. aging time for the material cured with both cycles.

Morphology

Figure 4 shows the SEM micrographs of the tensile fractured surface of samples of the material cured with the long cycle for 0, 24, and 240 h of thermal degradation.

The complete section of the specimens appears in Figure 4(a), (b), and (c) at $16\times$ magnification. The corresponding amplification of a centered characteristic zone appears in Figure 4(d), (e), and (f) at $100\times$ magnification.

A detailed analysis of the fractured surfaces of the micrographs at $16\times$ magnification allows identification of four characteristics zones. These zones are schematized in Figure 5.

Departing from the mirror-like region it can be seen fine lines or river markings oriented parallel to the direction of crack propagation, that is, these lines can be traced back enabling the defect or cause of failure to be identified. In our case from the Figure 4 it can be seen that the cause of failure is an air bubble on the surface. On the other hand, the aged specimens show a typical brittle fracture mode, as shown in Figure 4(b) and (c).

The fracture surfaces were observed at higher magnification (up to $5000\times$), and it can be noted that in the mirror-like region there are not significant items independently of the thermal degradation that the specimens were subjected. In the rough three-dimensional zone the folds are less depth and less distanced when thermal aging is increased.

The fracture surfaces for the specimens of the material cured with the short cycle present the same four characteristics zones showed in Figure 5, and also in the rough three-dimensional zone there is the same trend about the depth of the

folds and the separation between two folds with aging time that in the material cured with the long cycle.

DISCUSSION

Tensile Tests

The material cured with the long cycle presents better mechanical properties than the material cured with the short cycle; this fact may be due to the different tridimensional networks originated during the cure. When the cure is longer, the reaction is more complete and a higher conversion, α , is reached. In Figure 6, the two step-cure paths are shown superimposed on the time temperature transformation diagram (TTT) of this system.¹⁴ In this diagram are represented the isoconversion curves and the gelation and vitrification curves with their corresponding experimental points. The three critical temperatures for this system are $T_{g0} = -37^\circ\text{C}$, ${}_{\text{gel}}T_g \approx 30^\circ\text{C}$, and $T_{g\infty} \approx 150^\circ\text{C}$.

From this diagram it is observed that a slightly higher value of conversion is reached when the material is cured with the long cycle. It was established for this DGEBA/1,3-BAC epoxy system that the one-to-one correspondence between the glass transition temperature, T_g , and conversion is correctly described by a DiBenedetto's approach in the form used by Hale et al.,¹⁴ so even a small variation of the value of conversion in the region of high conversions involves significant changes of some properties of the material.

Thus, an increase in the activation energy of glass transition of the material that is well cured is expected, because crosslinking reactions are accompanied with a decrease in the segmental mobility of the polymer chains. This fact was experimentally confirmed: activation energies measured by DMA for the material cured both with the short and the long cycles were, respectively, 345.5 and 423.6 kJ/mol.¹⁵

On the other hand, for the material cured with the short cycle, the first hours of thermal degradation generate additional crosslinking and an increase in the glass transition temperature⁸ so, according to the Nielsen relationship,¹⁶ there is a decreasing in the molecular mass between crosslinks, M_c .

$$M_c = \frac{39000}{T_g - T_{g0}} \quad (1)$$

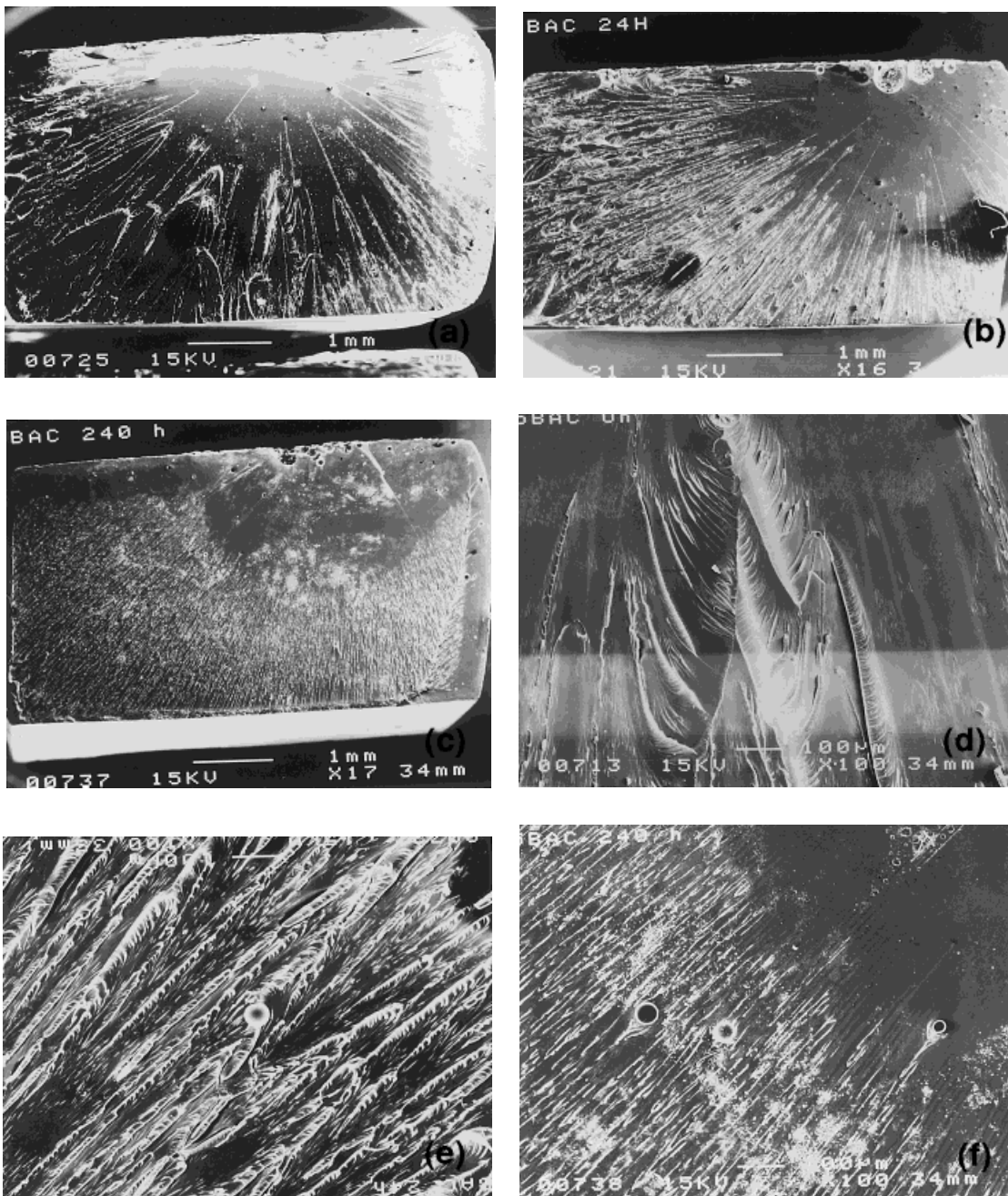


Figure 4 SEM micrographs showing the fracture surface morphologies of DGEBA/1,3-BAC specimens at different aging times (h): (a) 0 (16 \times); (b) 24 (16 \times); (c) 240 (17 \times); (d) 0 (100 \times); (e) 24 (100 \times); (f) 240 (100 \times).

Table II summarizes the values of T_g measured by DSC and the values of M_c in the first 1500 h of thermal degradation for the material cured with the short cycle. From this table it is observed that M_c approaches a constant value at high aging times. This variation can be taken as an indicator of the decrease of the rate factor R of the crosslink-

ing reaction, because this factor can be expressed as $R \approx K/t_e$, where K is a constant and t_e , the reaction time.¹⁷

Izod Impact Tests

The variation of the Izod impact strength with aging time is related with the variation of the

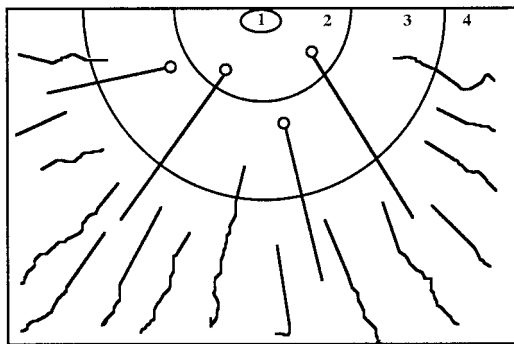


Figure 5 Four characteristic zones of the fractured surfaces: (1) a defect where failure is initiated; (2) a smooth mirror-like region; (3) a slightly less smooth area; (4) a rough three-dimension zone.

peak of β transition in $\tan \delta$ curve obtained by DMA. It is generally considered that β transition is very related with the impact properties of the materials when this transition is associated with motion about the chain backbone of a relatively small number of monomer units or with motion of side groups called crankshaft mechanism.¹⁸ The crankshaft mechanism needs an activation energy of about 11–15 kcal/mol and probably requires creation of free volume for rotation.¹⁹ The activation energy obtained for the β transition of this material cured with the short cycle was 53.4 kJ/mol or 12.8 kcal/mol.²⁰

Figure 7 illustrates the $\tan \delta$ of β transition for the material cured with the short cycle for the

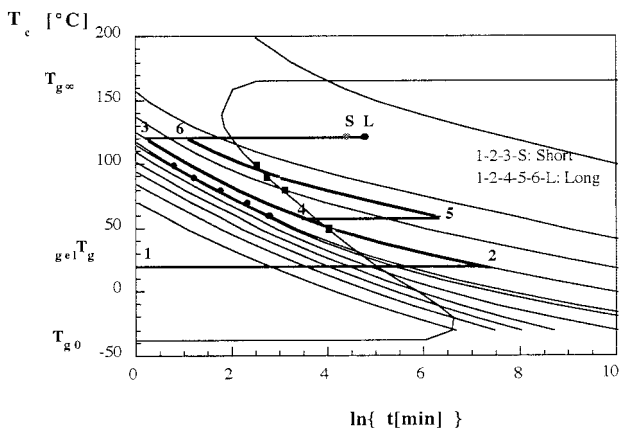


Figure 6 TTT isothermal cure diagram of DGEBA/1,3-BAC epoxy system. ■ and ● represent experimental times to vitrification and gelation, respectively. The two step-cure paths: 1–2–3–S represent the short cycle, and 1–2–4–5–6–L represent the long cycle.

Table II Molecular Mass between Crosslinks and Glass Transition Temperatures vs. Aging Time for the Material Cured with the Short Cycle

Time (h)	T_g (DSC) (°C)	M_c (mol/g)
0	139.0	221.7
480	145.0	214.4
984	146.6	212.5
1512	147.0	212.1

material without degradation and with 480 h of thermal aging.

Table III summarizes for this last material, the area and the height of the $\tan \delta$ curve for β transition vs. aging time. From these values can be observed a correlation between the decrease in the intensity of the β peak and a decrease of the Izod impact strength when thermal aging is increasing. Dynamic mechanical analysis shows, too, a significant decrease in the α peak, corresponding to the glass transition, and the existence of a secondary peak, α_2 , at high temperatures that is increasing and shifting to higher temperatures when thermal aging is increasing.²¹

Morphology

An examination of almost any epoxy fracture surface highlights the presence of a number of different regions. Also, in other polymers and metals there appear such regions. One way of explaining the formation of such zones is based in the variation of crack velocity during failure. It can be

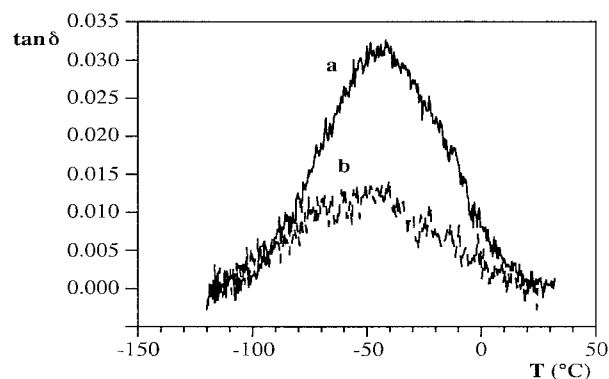


Figure 7 $\tan \delta$ vs. temperature for β transition for the material cured with the short cycle: (a) without degradation; (b) 480 h of aging time.

Table III Values of the Area and the Height of the $\tan \delta$ Curve for β Transition vs. Aging Time for the Material Cured with the Short Cycle

Time (h)	β Peak Area ($^{\circ}\text{C}$)	β Peak Height
0	2.03	0.032
480	0.91	0.013

shown that there will be a limiting velocity for crack propagation that is proportional to the velocity of sound in the material.²² A number of techniques are available for measuring the velocity of a crack in a brittle polymer.

The mirror-like region was found to correspond to the region of a slow crack growth. Parabolic markings in the direction of the defect are sometimes observed beyond the mirror-like region as in the micrograph of Figure 4(a), this region corresponds to the zone over which the crack was accelerating in an unstable manner. This parabolic markings are associated with the initiation of secondary cracks in front of the primary crack in this region.

When the crack has reached the maximum velocity, the crack branching and, therefore, a very rough three-dimensional fracture surface occurs.²³ The crack maximum velocity is a fraction of the sonic velocity of the material that is related with the Young modulus, E , and the density, ρ , of the material through the expression²⁴

$$v = \sqrt{\frac{E}{\rho}} \quad (2)$$

During degradation there is a reduction in the mass of samples and in the density of epoxy resins and, therefore, sonic velocity grows if E remains constant or slightly increases. The roughness diminution of the three-dimensional rough zone during degradation is suggesting that the crack had either stabilized at a velocity below the limiting value or else that the required acceleration zone is larger than the specimen dimensions. This roughness diminution for specimens more largely degraded is indicating a diminution in energy necessary to formation of fracture surfaces in accordance with diminution observed in the Izod impact strength.

CONCLUSION

Thermal degradation is a complex phenomenon that changes thermal and mechanical properties

of the material in an irreversible form. As aging time is increased, the properties of the material are changed in a significant way.

The loss of mechanical properties is manifested through the tensile and the Izod tests as an increase in the fragility of the material cured both with the short and the long cycles. However, the material cured with the long cycle presents better properties at any aging time. This better behavior for the material cured with the long cycle is explained by the great conversion and high crosslink density that this material reaches during the cure, as seen in the TTT diagram of this DGEBA/1,3-BAC epoxy system.

A good correlation was found between the decrease of the Izod impact strength and the decrease in the intensity of the peak of β transition in $\tan \delta$ curve obtained by DMA when thermal aging is increasing. This fact could agree with the supposition that the origin of the β transition is due to the motion of a crankshaft mechanism in the zone where the resin and the hardener are joined. It can be noted, too, there is a good correlation between the increase in the fragility of the material with aging time and the morphology of fractured surfaces observed by SEM, mainly in the rough three-dimensional zone.

This work was financially supported by Xunta de Galicia, through Grant XUGA 17201A92. The authors are grateful to SGAI, Universidade de A Coruña, for SEM analysis.

REFERENCES

1. B. Ellis, Ed., in *Chemistry and Technology of Epoxy Resins*, Blackie Academic and Professional, Glasgow, 1993, Chap. 1.
2. D. K. Hadad, in *Epoxy Resins. Chemistry and Technology*, 2nd ed., C. A. May, Ed., Marcel Dekker, New York, 1988, Chap. 14.
3. N. Grassie and M. I. Guy, *Polym. Degrad. Stabil.*, **14**, 125 (1986).
4. G. J. Knight and W. W. Wright, *Br. Polym. J.*, **21**(4), 303 (1989).
5. B. C. Burton, *J. Appl. Polym. Sci.*, **47**, 1821 (1993).
6. F. Rodríguez, *Principles of Polymer Systems*, 3rd ed., Hemisphere Publishers Co., New York, 1989, Chap. 11.
7. L. Barral, J. Cano, A. J. López, J. López, P. Nogueira, and C. Ramírez, *J. Therm. Anal.*, **45**, 1267 (1995).
8. L. Barral, J. Cano, A. J. López, J. López, P. No-

- gueira, and C. Ramírez, *Thermochim. Acta*, **269**, 253 (1995).
9. S. S. Saliba and J. A. Snide, in *International Encyclopedia of Composites*, Vol. 2, S. M. Lee, Ed., VCH Publishers, New York, 1990, p. 268.
 10. H. Jahn and P. Goetzky, *Epoxy Resins. Chemistry and Technology*, 2nd ed., C. A. May, Ed., Marcel Dekker, New York, 1988, Chap. 13.
 11. L. Barral, J. Cano, A. J. López, J. López, P. Nogueira, and C. Ramírez, *Polym. Int.*, **38**, 356 (1995).
 12. ASTM D638M-89, Annual Book of ASTM Standards, 1989.
 13. ASTM D256-89, Annual Book of ASTM Standards, 1989.
 14. L. Barral, J. Cano, A. J. López, J. López, P. Nogueira, and C. Ramírez, *J. Appl. Polym. Sci.*, **64**, 1553 (1996).
 15. L. Barral, J. Cano, A. J. López, J. López, P. Nogueira, and C. Ramírez, *XXV Reunión bienal Real Sociedad Española de Física. Resúmenes de las Comunicaciones*, R. Bravo and J. Salgado, Eds., Universidad de Santiago, Santiago de Compostela, 1995, p. 583.
 16. L. E. Nielsen, *J. Macromol. Sci.*, **c3**, 69 (1969).
 17. L. C. E. Struik, *Physical Aging in Amorphous Polymers and Other Materials*, Elsevier, Amsterdam, 1978, Chap. 6.
 18. A. V. Tobolsky, *Properties and Structure of Polymers*, Wiley, New York, 1960.
 19. G. E. Roberts and E. F. T. White, *The Physics of Glassy Polymers*, R. N. Harward, Ed., John Wiley & Sons, New York, 1973, Chap. 3.
 20. L. Barral, J. Cano, A. J. López, P. Nogueira, and C. Ramírez, *J. Therm. Anal.*, **41**, 1463 (1994).
 21. J. Cano, Ph.D. Thesis, Universidad de Santiago, 1995.
 22. I. M. Ward, *Mechanical Properties of Solid Polymers*, 2nd ed., Wiley, Chichester, UK, 1990, Chap. 12.
 23. W. J. Cantwell and H. H. Kausch, in *Chemistry and Technology of Epoxy Resins*, B. Ellis, Ed., Blackie Academic and Professional, Glasgow, 1993, Chap. 5.
 24. W. E. Gettys, F. J. Keller, and M. J. Skove, *Physics Classical and Modern*, McGraw-Hill, New York, 1989, Chap. 33.